Journal of Harbin Engineering University
ISSN: 1006-7043

Vol 44 No. 9
September 2023

Design and Development of Loads for the Final Wind Turbine

Kollibala Siva Rama Reddy S and Dr. Prashant Kumar Shrivastava
Department Mechanical Engineering,
Dr. A. P. J Abdul Kalam University Indore (M.P), India.

Abstract-This work discusses the need for a large number and long length of simulations to generate reliable load estimations, in addition to the inherent uncertainty in the simulation of loads using structural dynamics software. Loads data has substantial statistical variance, and we provide a methodology for extrapolation and quantile determination. In order to determine severe loads with a reasonable amount of uncertainty, it may be possible to further minimize the necessary numerical labor by using a stochastic process model for the dynamic reactions. We offer a method that allows for a non-Gaussian but nonetheless reasonably accurate answer. When everything is said and done, the turbine's extreme loads are computed accordance to the new IEC 61400-1 standard for safety regulations for wind turbines, and a comparison is made between loads derived from gust models and suitably extrapolated simulation extremes.
Keywords: Design, WTMB, Sustainable, Wind, Power

1. Introduction

Wind power, which is growing in popularity as a result of its advantages as a sustainable, environmentally friendly energy option, is a relatively recent addition to the global energy landscape. China, the global leader in renewable energy production, places a premium on wind power considering its aggressive push to promote "carbon peaking and carbon neutrality." In 2020, the IEA estimates that About 69 gigawatts (GW) of onshore wind power will have been constructed in China. The widespread use of wind power has opened promising new avenues for the expansion of the free market, but it has also presented several difficult obstacles, including those of ensuring the safety of the infrastructure, reducing costs, and ensuring enough supplies of electricity. On the one hand, the working environment is very complex, since wind turbines are often located in remote areas, Furthermore, the drive train of the turbine is extremely susceptible to the unpredictability and temporal variability of the wind. Wind turbines rely on their bearings, which are at the center of the drive train. In addition, a failure in the bearings may lead to a breakdown in the drive system or even equipment downtime, both of which will increase the cost of maintenance. However, this may be because of the constraints posed by wind turbines' high height, slow speed, and heavy load during operation. Since the bearings are difficult to inspect and remove, operating and maintaining wind power equipment is more complicated and costly.

As a result, having access to real-time fault diagnostics of wind power bearings is critical for maximizing the efficiency of wind power generation and preventing faults in advance.

2. Literature Review

Timothy Verstraeten et.al (2019) When it comes to transitioning to clean, renewable energy, wind farms play a key role. Placement in distant and hard places, however, increases transportation costs and reduces average wind speeds since there are so few appropriate sites. Improving the turbines' dependability is crucial for cutting down on repair costs. Understanding the loads that the turbine must act upon is crucial for a successful installation. However, equipment that must deal with dynamically changing multidimensional loads is rare and has received very little study. This is why we advocate for a multi-pronged approach to discovering the load spectrum in wind farms. Our approach is based on a combination of theoretical research carried out using programmed test rigs and practical research into real-world loading conditions obtained from records of frequent supervisory control and data collection. Methods are demonstrated for isolating operational regions within wind farm data and assigning those regions to individual loads. In addition, a system is

suggested that constantly improves the farm's control procedures without having to completely comprehend the loads that occur, allowing for further study into the load spectrum. Using data collected from a large number of studies, the causes of a gearbox failure are determined.

R Goyalet.al (2019) When intermittent energy sources are integrated at a higher rate into the system, stability issues arise. In order to control the frequency range of the power grid, hydraulic turbines' guiding vanes are commonly programmed to open and close automatically.This has resulted in more shutdown cycles than were originally planned for during regular turbine operation. Increased pressure fluctuations and flow field unsteadiness the lifespan of the turbine was drastically shortened when it was shut down. In this study, we report the results of tests conducted on a shutdown Francis turbine model at high head. The current research took into account the initial high load operating situation while shutting down the turbine. Sample rates of 40 Hz and 5 kHz were used to record information on PIV and pressure, respectively. In this study, we offer time-resolved velocity and pressure data to illustrate pressure variations and identify the mechanisms that give rise to unsteady flow in the draft tube.

Sharad Jain (2012) Despite using the most up-to-date design methods, wind-turbine gearboxes nevertheless have a high risk of premature failure. Failure of the gearbox, one of the most expensive components of a wind turbine, leads directly to higher energy prices. Bearings are the root cause of most issues with wind turbine gearboxes. Two of the most crucial parts are high-speed bearings and planet bearings, but they also have a high failure rate. Skidding in high-speed bearings and defect detection in planet bearings are two major topics covered in this dissertation. This dissertation begins with a discussion of sliding in high-speed bearings. High-speed bearings are susceptible to skidding because of the combination of low loads and high speeds at which they work. The failure caused by skidding often occurs much before the failure caused by conventional fatigue. However, under combined axial and radial loads and time-varying operating circumstances, the process of skidding in ball bearings is poorly understood. To study how angular-contact ball-bearings slide under axial and radial loads at various speeds over time, we construct a dynamic model. The model accounts for the gyroscopic effect. Skidding criteria established for thrust bearings are not transferable to those bearings operating under combined loading situations or time-varying speeds, as shown by the study. To foretell the occurrence of skidding under axial and mixed loading situations, we construct elementary analytical formulae. These equations need little in the way of processing resources and provide light on how various geometrical and operational aspects affect the skidding behavior.

Edward Hart et.al (2020) This study provides a comprehensive analysis of the literature and current practices around wind turbine main bearings. When it has to be replaced, the turbine rotor must usually be taken apart to access the main bearing and replaced. When put next to traditional power plants or even other bearings in the wind turbine's power train, this is a significant improvement(such the gearbox or generator), the loads and operating conditions experienced by wind turbine main bearings are very unique. The first is to document the present state of the art in main-bearing theory so that existing design and analysis methods can be assessed, and the second is to lay the framework for future research in this area. Wind turbine main bearing responses to typical rotor loads are discussed. After this comes tribological theory, which examines phenomena like lubrication, wear, and failure. Finally, methods for modeling bearings, problem diagnostics, and prognosis are discussed as they pertain to the main bearing.

Jan Helsen et.al (2016) This study analyzes how a wind turbine's high-speed gearbox stage functions when there is no electricity. The slip behavior of tapered roller bearings on high-speed shafts is studied in detail. It is demonstrated that the high-velocity shaft undergoes simultaneous torsional and bending deformation during the transient event. During torque reversals, roller slip caused by these unfavourable loading situations indicates that the applied load case may exceed the tapered roller bearings preload.

3. Calculating The Final Loads For Wind Turbine Design

The Hypothetical Windmill

As shown in Figure 1,The turbine's rotor has a nominal speed of 72 rpm and a diameter of 10 m. The hub of this three-bladed turbine is 17 meters above ground, and it spins freely in either direction downwind from the tower. All simulations were run using the commercially available ADAMS® programme coupled with the AeroDyn aerodynamic subroutines10. Extensive modal testing and component weighting in the system led to the development of the ADAMS model. Individual parts and whole assemblies were subjected to modal testing, and their weights were recorded. A bi-filar pendulum test and a weight measurement were used to ascertain the nacelle's inertia qualities. The weight of the blades was measured to pinpoint its center of gravity. Modal test configurations were utilized to fine-tune the ADAMS model such that it would reproduce the observed masses, centers of mass, and frequencies. There are 177 movable parts in this model. The tower's model consists of eight individual beams. The rotor's rotational DOF, shaft torsion at low speeds, and yaw are the other DOFs. The tower guy wires are modeled using nonlinear forces. The generator's torque-to-speed relationship was calculated using experimental data. Because of this, the model used in this investigation has been deemed verified and is likely to provide accurate load projections.

Figure 1 The National Wind Technology Center and the National Renewable Energy Laboratory are now conducting Phase III of the Unsteady Aerodynamics Experiment.

Two design Calculations

This research considered two IEC 61400-1 design conditions:

Table1 LoadCases

Design situation Load case	Wind speed (10 min aver.)	Power law exponent α	Target turb. intensity I_u*	Reference height
Operation at rated wind speed	14 m/s	0.2	17 %	16.8 m
Operation at cut-out wind speed	20 m/s	0.2	17 %	16.8 m
Parked at extreme wind speed	45 m/s	0.2	17 %	16.8 m

*Longitudinal turbulence component

- Generation of Energy

• Stopped (or idling) at a stop sign.

With no yaw limits and a constant 72 rpm, the wind turbine was believed to be at its most efficient operating condition for the Power Production design condition. the wind input for the design scenarios, the Parked design case additionally has a well-designed wind turbine with free yaw and a fixed rotor with blade #1 oriented vertically upwards. There is no correlation between wind input and wind turbine class, although the load scenarios are in line with Design Load Case 1.1 and 6.1 from IEC 61400-1. Instead of simulating a steady, high wind speed, the parked scenario depicts the wind as chaotic with a fixed mean speed.

The IEC 61400-1 Kaimal spectral model for three-dimensional wind turbulence was used to compute all loads. This contains the ratio of the standard deviations of the velocity components, integral length scales, and coherence decrements. One hundred simulations were run for each of the load situations. Each simulation ran for 610 seconds, but the first 10 seconds were skipped to avoid introducing noise from start-up transients. For the sake of further study, we have decided to keep the following primary signals and loads:

- Measured in meters per second, WindSpd
- Moment of in-plane bending at the root of the blade-B1_Moop
- Moment of in-plane bending at the root of the blade = B1_Mip
- YB_Fdw, the thrust in the longitudinal direction of the yaw bearing force
- Lateral yaw bearing force YB_Fcw
- YB_Mpitch, the yaw bearing pitching moment Momentum of yaw bearing rotation (YB_Mroll)The primary calculations for loads are described in Tables 2, 3, and 4. These fundamental statistical quantities are represented by their respective means, standard deviations, and coefficients of variation (COVs).

Table 2: 14 m/s Intensity Generation

Run statistics		WindSpd m/s	B1_Moop kNm	B1_Mip KNm	YB_Fdw kN	YB_Fcw kN	YB_Mpitch kNm	YB_Mroll kNm
Mean	Mean	14.10	0.86	0.74	2.35	-0.04	-3.09	-2.89
	St.dev	0.027	0.004	0.004	0.004	0.002	0.017	0.012
	COV	0.2%	0.5%	0.5%	0.2%	-6.2%	-0.6%	-0.4%
Stand Deviat.	Mean St.dev	2.18	0.65	0.92	0.50	0.16	1.27	0.32

	COV	0.052 2.4%	0.016 2.4%	0.002 0.2%	0.019 3.8%	0.006 3.7%	0.046 3.6%	0.016 5.2%
Mean cross. freq.	Mean St.dev COV	0.43 0.031 7.3%	3.20 0.053 1.6%	1.28 0.012 0.9%	2.43 0.039 1.6%	2.13 0.022 1.0%	2.37 0.086 3.6%	1.12 0.050 4.4%
Skewness	Mean St.dev COV	0.14 0.159 114.2%	0.05 0.032 62.1%	0.03 0.003 13.1%	-0.02 0.069 -301.7%	0.10 0.055 56.4%	-0.04 0.091 -237.8%	0.65 0.320 49.1%
Abs. Maxi-mum	Mean St.dev COV	21.79 0.873 4.0%	4.02 0.330 8.2%	2.91 0.109 3.8%	4.43 0.202 4.6%	0.74 0.105 14.1%	8.48 0.576 6.8%	3.90 0.094 2.4%

Table 3: Power Production at 20m/s

Run statisticss		**WindSpd m/s**	**B1_Moop kNm**	**B1_Mip KNm**	**YB_Fdw kN**	**YB_Fcw kN**	**YB_Mpitch kNm**	**YB_Mroll kNm**
Mean	Mean St.dev COV	20.14 0.035 0.2%	1.25 0.005 0.4%	0.81 0.003 0.4%	2.88 0.006 0.2%	-0.04 0.002 -4.4%	-3.50 0.013 -0.4%	-3.20 0.012 -0.4%
Stand. Deviat.	Mean St.dev COV	3.11 0.062 2.0%	0.82 0.020 2.4%	0.94 0.002 0.2%	0.79 0.030 3.8%	0.22 0.011 4.9%	1.571 0.057 3.6%	0.53 0.011 2.0%
Mean cross. freq.	Mean St.dev COV	0.51 0.035 6.9%	3.20 0.053 1.6%	1.40 0.020 1.4%	2.15 0.031 1.4%	2.18 0.018 0.8%	2.53 0.071 2.8%	0.79 0.037 4.7%
Skewness	Mean St.dev COV	0.137 0.131 0.960	0.01 0.046 466.8%	0.01 0.005 35.6%	0.79 0.030 3.8%	0.22 0.011 4.9%	0.05 0.084 158.0%	-0.53 0.088 -16.8%

Abs.	Mean	31.43	5.14	3.35	6.21	1.10	10.23	5.24
Maxi-	St.dev	1.259	0.498	0.160	0.379	0.161	0.821	0.223
mum	COV	4.0%	9.7%	4.8%	6.1%	14.7%	8.0%	4.2%

Table 4: The Numbers Stationed at a speed of 45 meters per second

Run statistics		**WindSpd m/s**	**B1_Moop KNm**	**B1_Mip kNm**	**YB_Fdw kN**	**YB_Fcw kN**	**YB_Mpitch kNm**	**YB_Mroll kNm**
Mean	Mean	45.31	7.90	1.40	8.36	-0.07	-7.86	-5.39
	St.dev	0.061	0.020	0.003	0.022	0.001	0.017	0.012
	COV	0.1%	0.2%	0.2%	0.3%	-1.1%	-0.2%	-0.2%
Stand. Deviat.	Mean	6.99	2.61	0.65	3.89	0.69	3.82	1.59
	St.dev	0.088	0.031	0.005	0.084	0.021	0.073	0.019
	COV	1.3%	1.2%	0.7%	2.2%	3.1%	1.9%	1.2%
Mean cross. freq.	Mean	0.77	1.78	4.48	1.67	2.24	2.21	1.18
	St.dev	0.035	0.053	0.058	0.033	0.017	0.037	0.032
	COV	4.6%	3.0%	1.3%	2.0%	0.8%	1.7%	2.7%
Skewness	Mean	0.13	0.32	0.17	0.22	-0.02	-0.20	-0.40
	St.dev	0.088	0.089	0.037	0.074	0.013	0.063	0.082
	COV	66.5%	27.8%	21.4%	33.7%	-67.0%	-32.0%	-20.5%
Abs. Maximum	Mean	71.81	20.10	4.30	25.38	3.08	25.24	12.61
	St.dev	2.909	1.594	0.302	2.013	0.294	2.014	0.839
	COV	4.1%	7.9%	7.0%	7.9%	9.5%	8.0%	6.7%

The mean crossing frequency of a signal is defined as the rate at which it crosses below its own mean value. The Extreme Value Type 1 (EV1) distribution is the asymptotic distribution of extremes (Gumbel), and its mean crossing frequency may be calculated by counting exponentially for big values.

Extreme Statistics

Under minimal assumptions, The Extreme Value Type 1 (EV1) distribution describes the expected frequency of extreme values as a whole. The EV1 distribution function equation in particular.

$$F(x;\alpha,\beta) = \exp(-\exp(-\alpha(x-\beta))) \quad (1)$$

Where α and β are the scale and location parameters respectively.

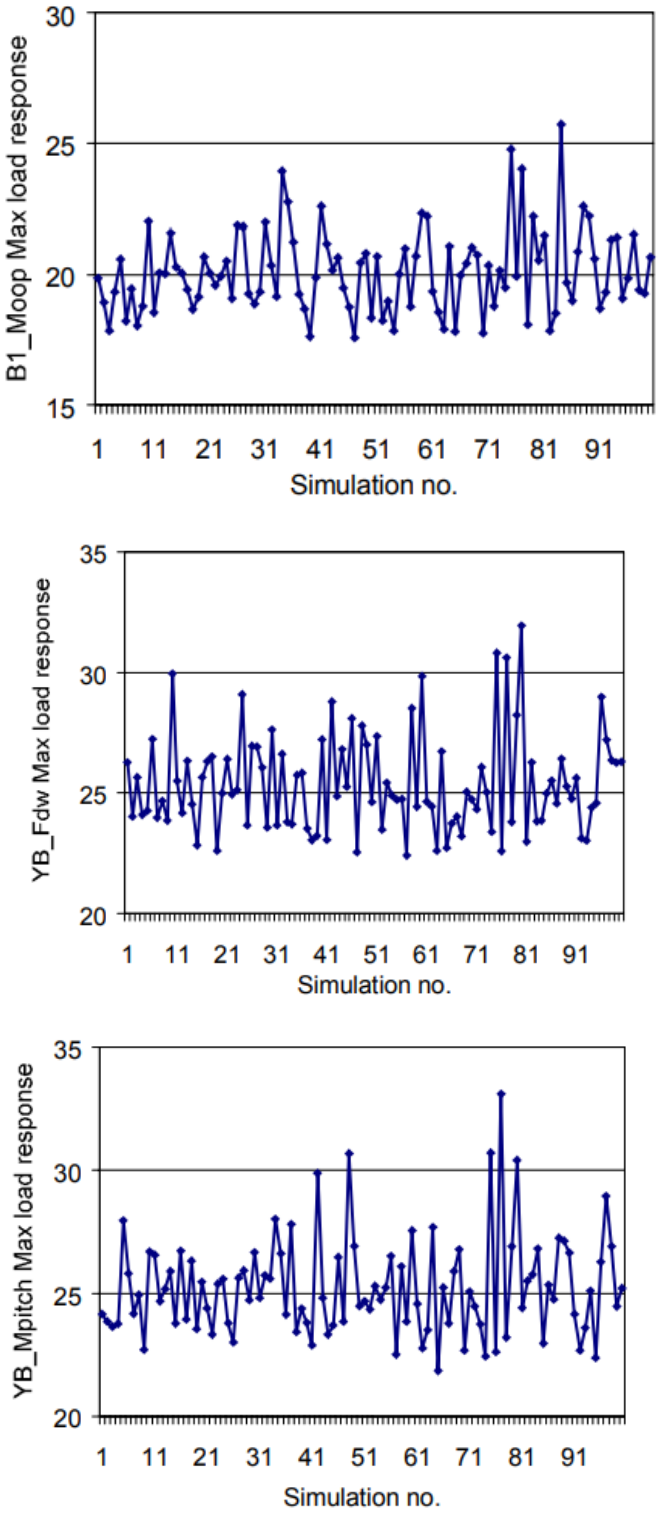

Figure 2: Simulations of severe loads over the course of 10 minutes when stopped at 45 m/s

Table 5: Type 1 Fitted Extreme Value Distribution Parameters for Extreme Loads

EV1-dist. From 100 time series		WindSpd m/s	B1_Moop kNm	B1_Mip kNm	YB_Fdw kN	YB_Fcw kN	YB_Mpitch kNm	YB_Mroll kNm
Power production -14 m/s	alfa	1.44	3.69	11.83	6.08	11.99	2.14	14.09
	beta	21.39	3.87	2.86	4.33	0.69	8.21	3.86
	mean	21.79	4.02	2.91	4.43	0.74	8.48	3.90
	st.dev	0.89	0.35	0.11	0.21	0.11	0.60	0.09
Power production -20 m/s	alfa	1.01	2.70	8.27	3.40	7.81	1.52	5.72
	beta	30.86	4.93	3.28	6.04	1.02	9.85	5.14
	mean	31.43	5.14	3.35	6.21	1.10	10.23	5.24
	st.dev	1.27	0.47	0.16	0.38	0.16	0.84	0.22
	alfa	0.44	0.79	4.10	0.62	4.26	0.64	1.50
Parked -	beta	70.50	19.37	4.16	24.46	2.95	24.34	12.22
45 m/s	mean	71.81	20.10	4.30	25.38	3.08	25.24	12.61
	st.dev	2.91	1.63	0.31	2.05	0.30	2.01	0.86

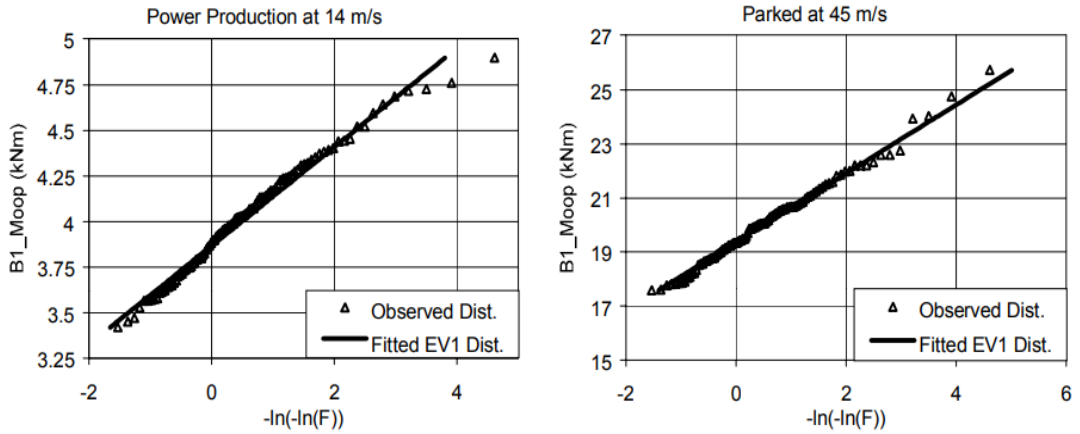

Figure 3: The highest value achievable in 100 independent 10-minute runs of severe out-of-plane bending moment

The probability-weighted moment (PWM) method will be utilized since it is a simple method for calculating the parameters of the EV1-distribution. The parameters of the fitted EV1-distributions, together with their means and standard deviations, were calculated using this method.

4. Conclusion

The submitted data shows that an aeroelastic algorithm fed with simulated turbulence produces statistically significant variance in its predictions of

ultimate loads. A large number of simulations are required for an accurate estimate, and this in turn depends on how the characteristic load is defined. It is concluded that turbulence response simulations, when used for the prediction of ultimate loads, must be coupled with statistical approaches. Using some basic extreme value data, we have attempted to determine normal load levels. Effectiveness and accuracy of a semi-analytical model for non-Gaussian process outliers have been shown. There are issues with comparing these loads to those specified by the IEC, but those issues are exclusive to this or similar wind turbines. Maximum loads during power generation are determined by running a normal turbulence model at both rated and cut-out wind speeds (load scenario 1.1). Extreme wind gusts from the IEC's load cases DLC 1.3, 1.6, 1.7, 1.8, and 1.9 are much less than the ultimate loads derived by extrapolating to 1 and 50-year occurrences.

Reference

[1] Verstraeten, Timothy & Nowe, Ann & Keller, Jonathan & Guo, Yi & Sheng, Shawn & Helsen, Jan. Fleetwide data-enabled reliability improvement of wind turbines. Renewable and Sustainable Energy Reviews. Vol. 109. Issue 22, Page No. 789-795, 2019 10.1016/j.rser.2019.03.019.

[2] R. Fuentes et.al "Detection of sub-surface damage in wind turbine bearings using acoustic emissions and probabilistic modeling" Vol. 21, Issue 4, Page No. 90-106, 2017

[3] R Goyal et.al "Experimental investigation on a high head Francis turbine model during shutdown operation" Vol. 65, Issue 43, Page No. 178-189, 2016,

[4] Sharad Jain "Skidding and Fault Detection in the Bearings of Wind-Turbine Gearboxes", Vol. 21, Issue 2, Page No. 1189-1196, 2012

[5] Edward Hart et.al "A review of wind turbine main bearings: design, operation, modelling, damage mechanisms and fault detection", Vol. 33, Issue 11, Page No. 145-153, 2018

[6] Helsen, Jan & Guo, Yi & Keller, Jonathan & Guillaume, Patrick. Experimental Investigation of Bearing Slip in a Wind Turbine Gearbox during a Transient Grid Loss Event. Wind Energy. Vol.19. Issue 4, Page No. 1189-1196, 2016.

[7] Whittle, Matthew & Shin, Won & Tavner, P.J. Improving wind turbine drivetrain bearing reliability through pre-misalignment. Wind Energy. Vol. 17. Issue 1, Page No. 191-197, 2014.

[8] AL-Bedhany, Jasim. Effect of Compression, Impact and Slipping on Rolling Contact Fatigue and Subsurface Microstructural Damage. Vol. 87, Issue 3, Page No. 1165-1172, 2020.

[9] Hart, E., Clarke, B., Nicholas, G., Kazemi Amiri, A., Stirling, J., Carroll, J., Dwyer-Joyce, R., McDonald, A., and Long, H.: A review of wind turbine main bearings: design, operation, modelling, damage mechanisms and fault detection, Wind Energ. Sci., Vol. 5, Issue 3, Page No. 105–124, 2020.

[10] Hussein BAKRI "Experimental and numerical study of soil-structure interaction subjected to cyclic-dynamic loading: Application to offshore wind turbine monopile foundation", Vol. 90, Issue 1, Page No. 1145-1152, 2021